Determining the presence of thin-wall regions at high-pressure areas in unruptured cerebral aneurysms by using computational fluid dynamics

Tomoaki Suzuki, MD[1,2], Hiroyuki Takao, PhD[1,3], Takashi Suzuki, MS[3], Yukinao Kambayashi, MD[1], Mitsuyoshi Watanabe, MD[1], Hiroki Sakamoto, MD[1], Issei Kan, MD[1], Kengo Nishimura, MD[1], Shogo Kaku, MD[1], Toshihiro Ishibashi, MD[1], Satoshi Ikeuchi, MD[1], Makoto Yamamoto, PhD[4], Yukihiko Fujii, PhD[2], Yuichi Murayama, MD[1]

[1]Department of Neurosurgery, The Jikei University School of Medicine, Tokyo, Japan.
[2]Department of Neurosurgery, Brain Research Institute, Niigata University, Niigata, Japan.
[3]Graduate School of Mechanical Engineering, Tokyo University of Science, Tokyo, Japan.
[4]Department of Mechanical Engineering, Tokyo University of Science, Tokyo, Japan.

Corresponding author: Yuichi Murayama, MD
Department of Neurosurgery, The Jikei University School of Medicine
3-25-8 Nishi-Shinbashi, Minato-ku, Tokyo 105-8461, Japan
Tel: +81-3-3433-1111 ex.3461; Fax: +81-3-3459-6412; E-mail: ymurayama@jikei.ac.jp

Itemized list of tables and figures: one table and five figures

Disclosure of funding
This work was partially supported by a research grant from Siemens Japan K.K.
Y.M. received grants from Siemens Japan K.K., Stryker Japan K.K., and ASAHI INTECC.
H.T. received grants from Siemens Japan K.K. and NTT docomo.

Abstract

Background: Thin-wall regions (TWRs) of cerebral aneurysms are at high risk of rupture, and careful attention should be paid during surgical procedures. Despite this, an optimal imaging technique to estimate TWRs has not been established. Previously, pressure elevation at TWRs was reported using computational fluid dynamics (CFD), although not fully evaluated.

Objectives: To investigate the possibility of predicting aneurysmal TWRs at high-pressure areas by using CFD.

Methods: Fifty unruptured middle cerebral artery aneurysms were analyzed. Spatial and temporal maximum pressure (Pmax) areas were determined using a fluid flow formula under pulsatile blood flow conditions. Intraoperatively, TWRs of aneurysm domes were identified as reddish areas relative to the healthy normal MCAs; 5 neurosurgeons evaluated and divided these regions according to Pmax area and TWR correspondence. Pressure difference (Pd) was defined as the degree of pressure elevation on the aneurysmal wall at Pmax and was calculated by subtracting the average pressure (Pave) from the Pmax and dividing by the dynamic pressure at the aneurysm inlet side for normalization.

Results: In 41 of the 50 cases (82.0%), the Pmax areas and TWRs corresponded. Pd values were significantly higher in the correspondence group than in the non-correspondence group ($p = 0.008$). A receiver operating characteristic curve demonstrated that Pd accurately predicted TWRs at Pmax areas (area under the curve: 0.764 [95% confidence interval: 0.574–0.955]; cutoff value: 0.607; sensitivity: 66.7%; specificity 82.9%).

Conclusions: A high Pd may be a key parameter for predicting TWRs in unruptured cerebral aneurysms.

Running title: Thin-wall regions in unruptured aneurysms

Key words: Computational fluid dynamics, pressure, thin-wall region, aneurysm

Introduction

Cerebral aneurysms carry a risk of life-threatening rupture and are associated with high rates of mortality and morbidity.[1] Aneurysm rupture is thought to occur at thin-wall regions (TWRs) caused by degeneration resulting from abnormal hemodynamic stress.[2-4] These TWRs have the potential risk of rupture during surgical treatment, and are frequently observed on the daughter sacs of aneurysms. Although imaging modalities for evaluation of cerebral aneurysms have improved recently,[5,6] these methods do not directly evaluate the condition of the aneurysm wall. Contrary to expectations, thick-wall regions may be observed on the daughter sac and may not have a high risk for rupture. Thus, evaluation of the wall condition may be important to predict the risk of rupture during surgical treatment. Computational fluid dynamics (CFD) analyses have been applied for risk analysis of rupture or growth mechanisms in cerebral and unruptured intracranial aneurysms (UIAs). Several parameters, such as wall shear stress (WSS), pressure, and energy loss (EL), have been studied with regard to anticipation of eventual rupture of UIAs [7-9]. Pressure, a basic hemodynamic parameter within the aneurysm wall, is directed perpendicularly to the wall surface, and although previous studies have reported pressure elevation at TWRs, this finding has not been fully evaluated.[10,11] This study aimed to evaluate aneurysmal TWRs using CFD modeling.

Methods

Source of the data and imaging

This retrospective study included 50 unruptured middle cerebral artery (MCA) aneurysm cases in 32 women and 18 men (mean age, 62.7 ± 8.73 years; mean aneurysm size, 5.99 ± 1.97 mm) treated by neck clipping at our institution between March 2009 and May 2015; in all cases, operators could observe the aneurysm wall surface directly and clearly. Only patients with unruptured saccular aneurysms and available intraoperative video files, three-dimensional (3D) digital subtraction angiography (DSA), or 3D computed tomography angiography (CTA) data were included. Aneurysms that were dissecting, fusiform, or clipped after coil embolization were excluded. Ruptured aneurysms were also excluded because of the impaired visualization of the aneurysm wall.

The study protocol was approved by the local ethics committee of our institution.

CFD modeling

Blood vessel geometry was extracted from CTA and DSA images of the head via manual

cropping and image thresholding; this information was subsequently converted to a triangulated surface using Real Intage (Cybernet Systems, Tokyo, Japan), which was then used to generate an unstructured computational volumetric mesh. This mesh mainly comprised tetrahedrons, along with several prism element layers near the wall surface to increase the analytic precision of the boundary layer. After assuming a pulsatile laminar flow, no pressure at the blood vessel outlet, Newtonian fluid dynamics, and rigid blood vessel walls with nonslip conditions, blood flow along the computational mesh was simulated using Navier–Stokes equations. A commercial software package (ANSYS ICEM CFD 14.5, ANSYS Inc., Canonsburg, PA, USA) was used to generate mesh and fluid dynamics. Additional details regarding computational fluid dynamics modeling details are provided in Figure 1. The fluid meshes were composed of 997,311 elements and 486,217 nodes. The analysis domain encompassed the aneurysm inlet side to the outlet side, including the aneurysm dome. The grid independence test was performed on aneurysm models (see Figures and Table, Supplemental Digital Content, which demonstrates the results of grid independence test).

Analysis of hemodynamic parameters of the aneurysm wall

Maximum pressure (Pmax) was calculated as the highest area of pressure at the aneurysm wall, both spatially and temporally. Average pressure (Pave) was also calculated as the mean value of pressure in the domain. For comparisons of aneurysms, the pressure difference (Pd) was defined as the degree of pressure elevation at the aneurysm wall at the Pmax area by subtracting Pave from Pmax. This value was divided by the dynamic pressure at the aneurysm inlet side for normalization.

$$Pressure\ difference = \frac{Pmax - Pave}{\frac{1}{2}\rho Vin^2}$$

Pmax: maximum pressure [Pa], Pave: average pressure [Pa],
ρ: 1100 [kg/m^3], Vin: mean velocity of the aneurysm inlet [m/s]

At the Pmax area, we also assessed the WSS, frictional force of blood flow along the aneurysm wall. Calculations included the minimum WSS (WSSmin) as the lowest WSS value, time average WSS (TAWSS) as the mean WSS value, and normalized WSS as the WSSmin value divided by the mean WSS of the vessel wall at the inlet side.

Semiquantitative assessment of thin-wall regions of aneurysms

Clipping was performed using the ZEISS OPMI PENTERO 900 (Zeiss, Oberkochen, Germany) or OLYMPUS OME-8000 (OLYMPUS, Tokyo, Japan) to treat all MCA aneurysms. Intraoperative video recording was performed in all cases. Based on previous studies,[3,10,12] the thin-wall surfaces of the aneurysms were defined as a region having red color, translucence, and extreme wall thinness, compared with healthy areas of the MCA. Five neurosurgeons reviewed the intraoperative videos and scored the aneurysm walls on a 5-point scale to compare the Pmax point of the aneurysm dome with those of normal MCAs (Figure 2). The observers were not provided the CFD maps. They only noted the intraoperative view and the Pmax point which is indicated by an asterisk. We defined thin-walled areas as those having average scores of 4 or more points.

Statistical analysis

Continuous data are shown as means ± standard deviations (SD). Statistical analysis was performed using R (ver. 3.1.3; R Project for Statistical Computing, Vienna, Austria). An overall significance level of $P < 0.05$ was adopted. We evaluated the normality of all parameters using the Kolmogorov–Smirnov test. We used the t-test to analyze parameters, for which the normality assumption could not be rejected at a significance level of 0.05 and the Mann–Whitney test to analyze parameters for which normality could not be established. To assess the accuracy of TWR predictions, a receiver operating characteristic (ROC) analysis was performed to determine the area under the curve (AUC), cutoff value, sensitivity, and specificity.

Results

In 41 of 50 (82.0%) cases, the Pmax area corresponded to the TWRs (Figures 3AB); in 9 cases, the Pmax area did not correspond to the TWR (Figure 4). Comparisons of sex, age, size, and hemodynamic aneurysm parameters between the correspondence and non-correspondence groups are shown in the Table. The Pd of the correspondence group was significantly higher than that of the non-correspondence group ($p = 0.008$, Figure 5A); however, the WSSmin, TAWSS, and NWSS did not significantly differ. The ROC curve demonstrated that the Pd value could accurately predict TWRs (AUC: 0.764 [95% confidence interval 0.574–0.955]; cut-off value: 0.607; sensitivity: 66.7%; specificity: 82.9%) (Figure 5B).

Discussion

Our study focused on pressure, a basic hemodynamic parameter of the aneurysm wall. Most

CFD studies have attempted to elucidate the involvement of WSS in aneurysm rupture; despite this, information on this involvement remains unclear, whereas few studies have evaluated pressure in the aneurysm wall.[10,11] Previously, Kadasi et al. reported the co-localization of TWRs with areas of low WSS.[10] That study included a small number of cases and also reported focal pressure elevation at TWRs. Although aneurysm rupture is thought to occur in TWRs, only a few reports have evaluated these regions.[3,10,12] In our study, we assessed 50 aneurysm wall surfaces using intraoperative videos and investigated the correlation between pressure elevation and TWRs in greater detail. Most Pmax areas corresponded with TWRs (82.0%). Furthermore, we defined Pd by using a formula for calculating the degree of pressure elevation in the aneurysm wall at the Pmax area, and when comparing aneurysms, a higher Pd value predicted a TWR at the Pmax area. Shojima et al. reported that local pressure elevation resulting from a bloodstream impacting force was not sufficient to contribute to aneurysm rupture.[13] However, in that study, the authors did not appropriately evaluate the aneurysm wall surface. Biologically, pressure elevation has been estimated to induce endothelial damage and activate inflammatory cascades, hypertrophy, migration, and extracellular matrix imbalances.[14] Accordingly, pressure is a non-negligible hemodynamic force on the aneurysm wall. Our study presents a preliminary investigation of the correlation between high-pressure areas and TWRs of aneurysms.

According to the results of our study, although no significant correlation was observed between the relevant WSS parameters and TWRs, a relatively higher WSS corresponded with TWRs at the Pmax area. Although we only focused on TWRs in Pmax areas, these results were different from those reported by Kadasi et al. Cebral et al. described a high WSS and impingement flow zone at the rupture site.[15] These Pmax areas were almost always observed at the first or second impact zone after the impact at the aneurysm neck, suggesting that the hemodynamic parameters of TWRs observed in our study are similar to those at the rupture site, as described by Cebral et al. Estimating the presence of TWRs is very useful when treating cerebral aneurysms not only during open surgery, but also during endovascular surgery, an increasingly common treatment that is performed depending on aneurysm wall surfaces. In the cases in which aneurysm blebs with high Pd values were located near the neck, along with a thin, reddish wall, early and careful treatment should be considered,[16,17] as these morphological configurations have been associated with a high risk of rupture.

Limitations

The present study has some limitations. First, we only evaluated aneurysms that were located

in the MCA because this vessel facilitates complete visualization of the aneurysm dome surface relative to other aneurysm locations, such as the anterior communicating artery and internal carotid artery. Future studies should evaluate aneurysms in other locations. Second, the boundary conditions were uniform across all cases, whereas in practice, these conditions may vary among cases. For patient-specific analysis, boundary conditions could be established using magnetic resonance imaging and echo imaging, if available. Third, the vessel walls were also assumed to be rigid, whereas in practice, they may deform to a different degree during the cardiac cycle.

Fourth, the TWR evaluation method was relatively subjective. The exact wall thickness was not measured because of its aneurysmal nature. Histopathological validation will be needed. Finally, the present study performed retrospective analyses of a limited number of cases. Additional prospective and multicenter studies are warranted to clarify the correlations between hemodynamic parameters and TWRs of aneurysms.

Conclusions

Areas of maximum pressure may be important markers of TWRs in unruptured cerebral aneurysms. By calculating the Pd value for each aneurysm type by using CFD, estimating the accuracies of predictions of the presence of TWRs may be possible. In the surgical treatment of cerebral aneurysms, high Pd provides useful information for avoiding the risk of rupture that may result in fatal outcomes.

References

[1] Wermer MJ, van der Schaaf IC, Algra A, Rinkel GJ. Risk of rupture of unruptured intracranial aneurysms in relation to patient and aneurysm characteristics: an updated meta-analysis. *Stroke*. 2007;38:1404-1410.

[2] Frösen J, Piippo A, Paetau A, Kangasniemi M, Niemelä M, Hernesniemi J, et al. Remodeling of saccular cerebral artery aneurysm wall is associated with rupture histological analysis of 24 unruptured and 42 ruptured cases. *Stroke*. 2004;35:2287-2293.

[3] Song J, Park JE, Kim HR, Shin YS. Observation of cerebral aneurysm wall thickness using intraoperative microscopy: clinical and morphological analysis of translucent aneurysm. [Published online ahead of print February 5, 2015]. *Neurol Sci*. 2015. http://link.springer.com/article/10.1007/s10072-015-2101-9. Accessed March 11, 2015.

[4] Xiang J, Natarajan SK, Tremmel M, et al. Hemodynamic-morphologic discriminants for intracranial aneurysm rupture. *Stroke*. 2011;42:144-152.

[5] Edjlali M, Gentric JC, Régent-Rodriguez C, et al. Does aneurysmal wall enhancement on vessel wall MRI help to distinguish stable from unstable intracranial aneurysms? *Stroke*. 2014;45:3704-3706.
[6] Hayakawa M, Maeda S, Sadato A, et al. Detection of pulsation in ruptured and unruptured cerebral aneurysms by electrocardiographically gated 3-dimensional computed tomographic angiography with a 320-row area detector computed tomography and evaluation of its clinical usefulness. *Neurosurgery*. 2011;69:843-851.
[7] Takao H, Murayama Y, Otsuka S, et al. Hemodynamic differences between unruptured and ruptured intracranial aneurysms during observation. *Stroke.* 2012;43:1436-1439.
[8] Meng H, Tutino VM, Xiang J, Siddiqui A. High WSS or low WSS? Complex interactions of hemodynamics with intracranial aneurysm initiation, growth, and rupture: toward a unifying hypothesis. *AJNR Am J Neuroradiol*. 2014;35:1254-1262.
[9] Miura Y, Ishida F, Umeda Y, et al. Low wall shear stress is independently associated with the rupture status of middle cerebral artery aneurysms. *Stroke*. 2013;44:519-521.
[10] Kadasi LM, Dent WC, Malek AM. Colocalization of thin-walled dome regions with low hemodynamic wall shear stress in unruptured cerebral aneurysms. *J Neurosurg*. 2013;119:172-179.
[11] Kono K, Fujimoto T, Shintani A, Terada T. Hemodynamic characteristics at the rupture site of cerebral aneurysms: a case study. *Neurosurgery*. 2012;71:E1202-1208.
[12] Kadasi LM, Dent WC, Malek AM. Cerebral aneurysm wall thickness analysis using intraoperative microscopy: effect of size and gender on thin translucent regions. *J Neurointerv Surg*. 2013;5:201-206.
[13] Shojima M, Oshima M, Takagi K, et al. Role of the bloodstream impacting force and the local pressure elevation in the rupture of cerebral aneurysms. *Stroke*. 2005;36:1933-1938.
[14] Anwar MA, Shalhoub J, Lim CS, Gohel MS, Davies AH. The effect of pressure-induced mechanical stretch on vascular wall differential gene expression. *J Vasc Res*. 2012;49:463-478.
[15] Cebral JR, Mut F, Weir J, Putman C. Quantitative characterization of the hemodynamic environment in ruptured and unruptured brain aneurysms. *AJNR Am J Neuroradiol.* 2011;32:145-151
[16] Park J, Woo H, Kang DH, Kim Y, Baik SK. Ruptured intracranial aneurysms with small basal outpouching: Incidence of basal rupture and results of surgical and endovascular treatments. *Neurosurgery*. 2012;71:994-1001.
[17] Kang DH, Goh DH, Baik SK, Park J, Kim YS. Morphological predictors of intraprocedural rupture during coil embolization of ruptured cerebral aneurysms: do small basal

outpouchings carry higher risk? *J Neurosurg*. 2014;121:605-612.

Figure legends

Figure 1. Computational fluid dynamics (CFD) model. Inlet mass flow rate (A); CFD analysis condition (B) and domain (C).

Figure 2. Three examples of analytical computational fluid dynamics (CFD). Left: The Pmax point of the aneurysm dome is indicated by an asterisk. Right: Intraoperative view. Neurosurgeons scored the area indicated by an asterisk on a 5-point scale relative to the normal, healthy vessel. The average aneurysm wall scores are (A) 5.0, (B) 3.4, and (C) 2.6.

Figures 3A,B. Pressure distributions (left), pressure difference (PD) (middle) and intraoperative views (right) of six representative aneurysms. The maximum pressure area (Pmax) (blue arrow) correspond to TWRs of the aneurysm domes.

Figure 4. Three representative aneurysms in the non-correspondence group. The maximum pressure areas (Pmax) (blue arrow) do not correspond to TWRs of these aneurysms.

Figure 5. (A) Comparison of pressure difference (Pd) values between the correspondence and non-correspondence groups. (B) Receiver operating characteristic curve of Pd for predicting TWRs.

Supplemental Digital Content

Supplemental Digital Content. Figures and table that demonstrates the results of grid independence test. doc

Supplement legends

Supplemental Digital Content. Figure 1 illustrates the total number of elements in each grid model and cut planes of the internal carotid artery (ICA) (left), pressure distribution (middle) and pressure difference (Pd) (right). The maximal pressure (Pmax) (blue dot) is the same in each condition. Figure 2 demonstrates the conditions of systolic peak and end diastolic mass flow rate (MFR). Table demonstrates the results of Pd in each condition. The error range is shown in parentheses (compared with Pd value in the grid model with the element number as 2,210,533 at peak systolic phase); all of them are less than 5%.

A

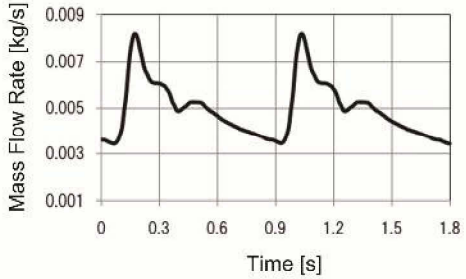

B

Density, ρ	1100 [kg/m^3]
Viscosity	0.0036 [Pa·s]
Computational model	Laminar (Re is approximately 500)
Simulation time step	0.0005 [s]
Inlet condition	Cardiac beat condition (Mass flow rate)
Outlet condition	Fixed static pressure (0 [Pa])

C

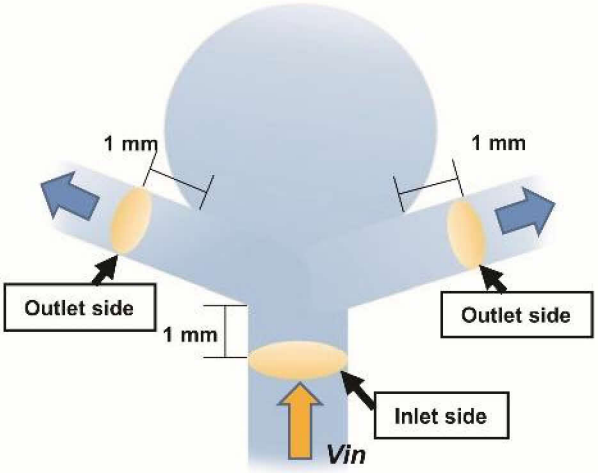

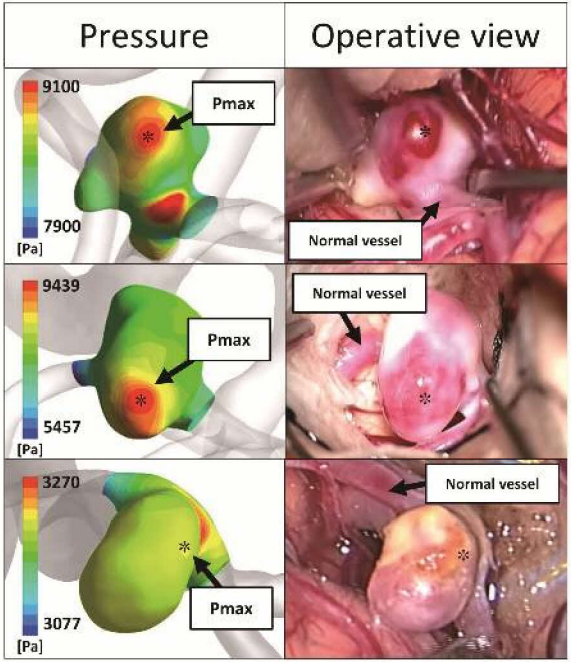

5	red
4	light red
3	same
2	light white or yellow
1	white or yellow

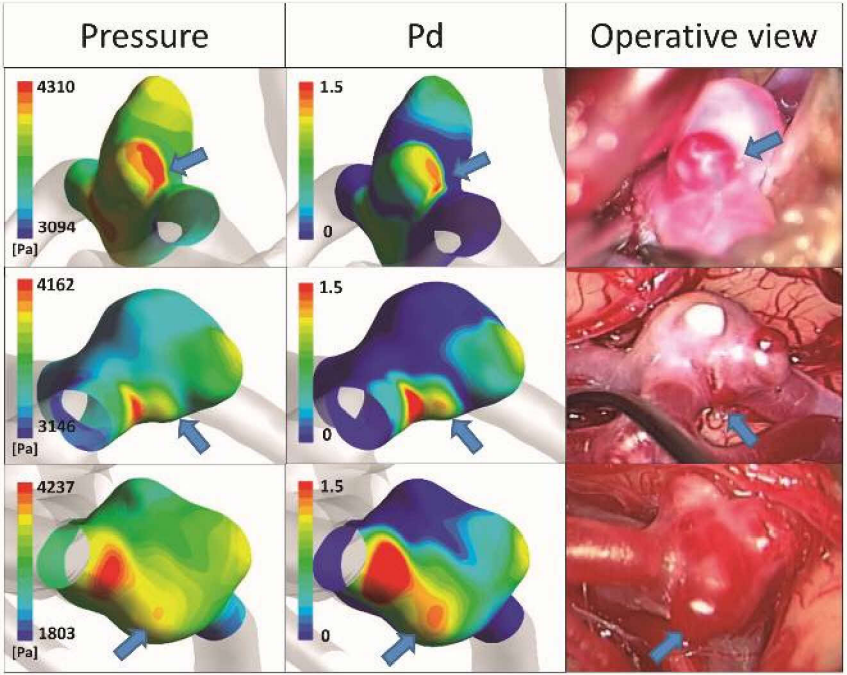
Pressure
Pd
Operative view
4310
3094
[Pa]
1.5
0
4162
3146
[Pa]
1.5
0
4237
1803
[Pa]
1.5
0

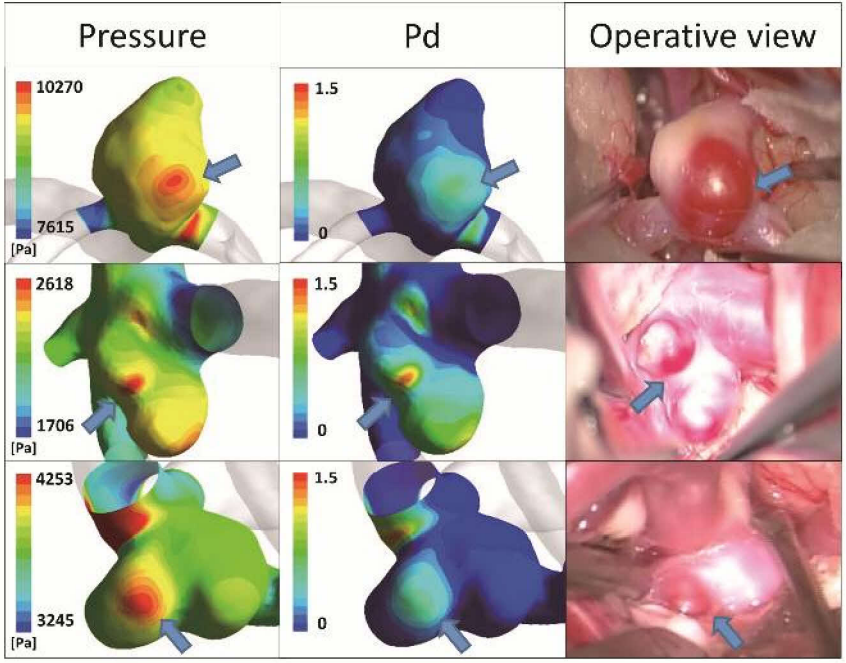
Pressure
Pd
Operative view
10270
7615
[Pa]
1.5
0
2618
1706
[Pa]
1.5
0
4253
3245
[Pa]
1.5
0

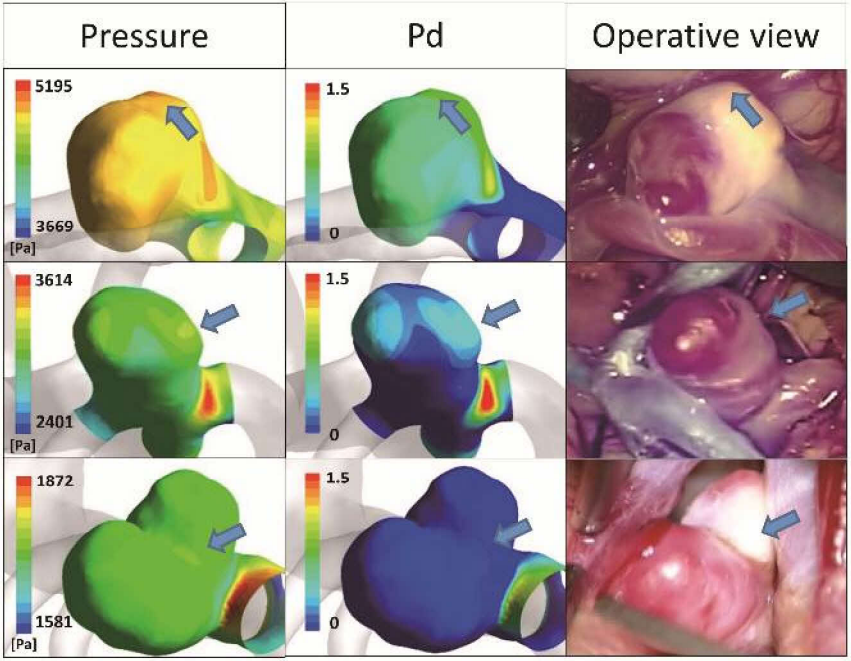
Pressure
Pd
Operative view
5195
3669
[Pa]
1.5
0
3614
2401
[Pa]
1.5
0
1872
1581
[Pa]
1.5
0

A

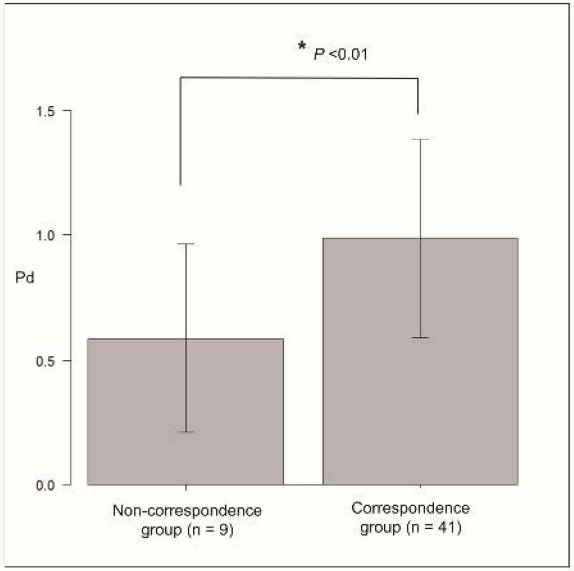
* P <0.01
1.5
1.0
0.5
0.0
Pd
Non-correspondence group (n = 9)
Correspondence group (n = 41)

B

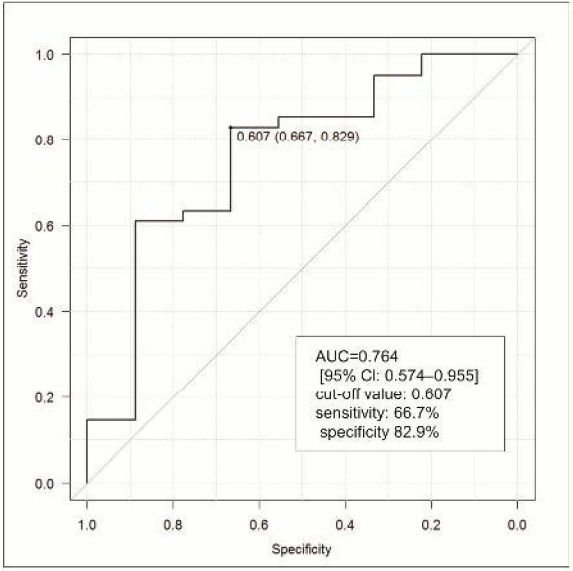
1.0
0.8
0.6
0.4
0.2
0.0
Sensitivity
0.607 (0.667, 0.829)
AUC=0.764
[95% CI: 0.574–0.955]
cut-off value: 0.607
sensitivity: 66.7%
specificity 82.9%
1.0
0.8
0.6
0.4
0.2
0.0
Specificity

Table

Table.

Statistical comparison of aneurysms between the correspondence and non-correspondence groups.

	Non-correspondence group (n = 9) *	Correspondence group (n = 41) *	*P value*†
Sex			0.054
Male	6 (33.3%)	12 (66.7%)	
Female	3 (9.3%)	29 (90.7%)	
Age, y	61.5 (± 10.12)	63.0 (± 8.52)	0.658
Size, mm	5.45 (± 1.43)	6.11 (± 2.06)	0.441
Vin, m/s	0.764 (± 0.435)	0.863(± 0.332)	0.445
WSSmin, Pa	2.720 (± 3.870)	3.881 (± 3.113)	0.064
TAWSS, Pa	6.068 (± 8.904)	9.914 (± 11.301)	0.113
NWSS	0.340 (± 0.326)	0.539 (± 0.355)	0.096
Pave, Pa	3522 (± 2266)	3878 (± 2412)	0.667
Pmax, Pa	3859 (± 2739)	4340 (± 2644)	0.495
Pd	0.585 (± 0.377)	0.986 (± 0.397)	0.008

* Values are shown as means and standard deviations or numbers and percentages.

† t test, Mann–Whitney U test; a P value <0.05 was considered statistically significant.

Abbreviations: Vin: mean velocity of the aneurysm inlet; WSS, wall shear stress; min, minimum; TAWSS, time average WSS; NWSS, normalized WSS; Pave, average pressure; Pmax, maximum pressure; Pd, pressure difference

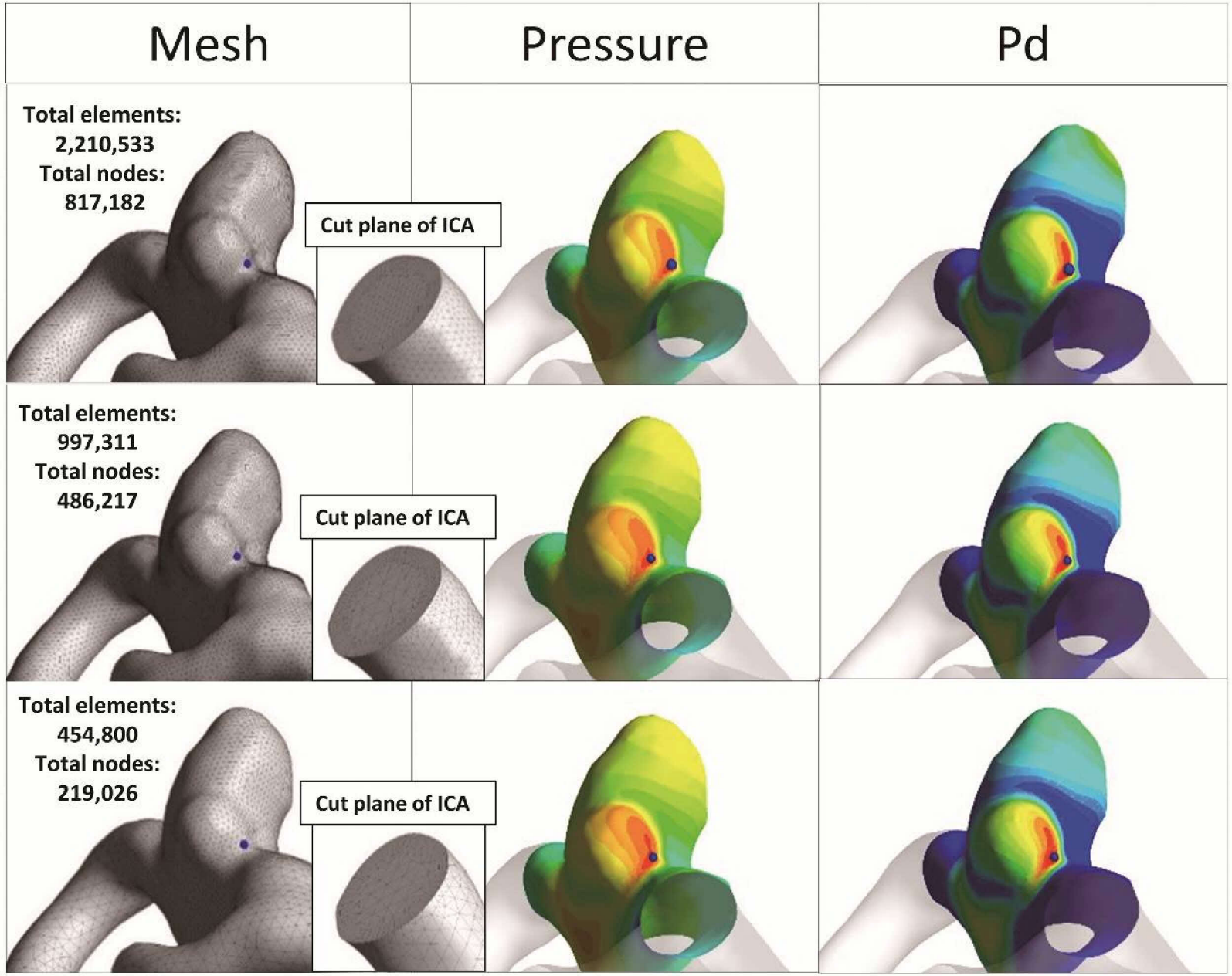
Mesh
Pressure
Pd
Total elements:
2,210,533
Total nodes:
817,182
Cut plane of ICA
Total elements:
997,311
Total nodes:
486,217
Cut plane of ICA
Total elements:
454,800
Total nodes:
219,026
Cut plane of ICA
Blue dot is Pmax

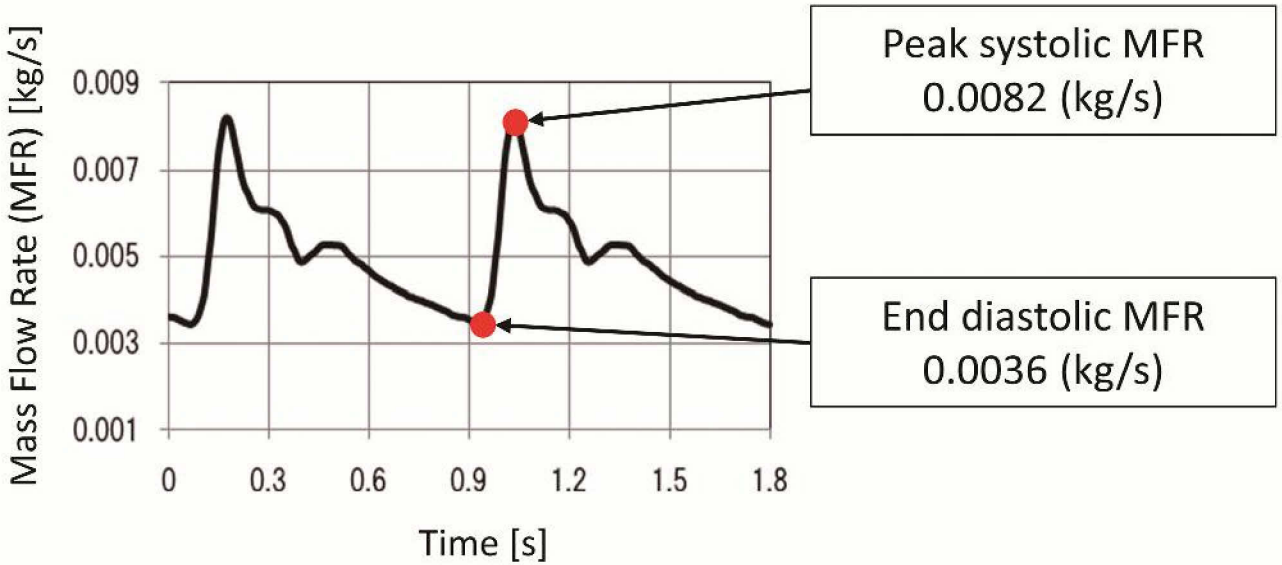
Mass Flow Rate (MFR) [kg/s]
0.009
0.007
0.005
0.003
0.001
0
0.3
0.6
0.9
1.2
1.5
1.8
Time [s]
Peak systolic MFR
0.0082 (kg/s)
End diastolic MFR
0.0036 (kg/s)